

The power spectrum and bispectrum of SDSS DR11 BOSS galaxies II: cosmological interpretation

Héctor Gil-Marín^{1*}, Licia Verde^{2,3,4}, Jorge Noreña^{2,5}, Antonio J. Cuesta²,
Lado Samushia¹, Will J. Percival¹, Christian Wagner⁶, Marc Manera⁷,
Donald P. Schneider^{8,9}

¹ *Institute of Cosmology & Gravitation, University of Portsmouth, Dennis Sciama Building, Portsmouth PO1 3FX, UK*

² *Institut de Ciències del Cosmos, Universitat de Barcelona, IEEC-UB, Martí i Franquès 1, 08028, Barcelona, Spain*

³ *ICREA (Institució Catalana de Recerca i Estudis Avançats), Passeig Lluís Companys, 23 08010 Barcelona - Spain*

⁴ *Institute of Theoretical Astrophysics, University of Oslo, Norway*

⁵ *Department of Theoretical Physics and Center for Astroparticle Physics (CAP), 24 quai E. Ansermet, CH-1211 Geneva 4, CH*

⁶ *Max-Planck-Institut für Astrophysik, Karl-Schwarzschild Str. 1, 85741 Garching, Germany*

⁷ *University College London, Gower Street, London WC1E 6BT, UK*

⁸ *Department of Astronomy and Astrophysics, The Pennsylvania State University, University Park, PA 16802, USA*

⁹ *Institute for Gravitation and the Cosmos, The Pennsylvania State University, University Park, PA 16802, USA*

4 August 2014

ABSTRACT

We examine the cosmological implications of the measurements of the linear growth rate of cosmological structure obtained in a companion paper from the power spectrum and bispectrum monopoles of the Sloan Digital Sky Survey III Baryon Oscillation Spectroscopic Survey Data, Release 11, CMASS galaxies. This measurement was of $f^{0.43}\sigma_8$, where σ_8 is the amplitude of dark matter density fluctuations, and f is the linear growth rate, at the effective redshift of the survey, $z_{\text{eff}} = 0.57$. In conjunction with Cosmic Microwave Background (CMB) data, interesting constraints can be placed on models with non-standard neutrino properties and models where gravity deviates from general relativity on cosmological scales. In particular, the sum of the masses of the three species of the neutrinos is constrained to $m_\nu < 0.49$ eV (at 95% confidence level) when the $f^{0.43}\sigma_8$ measurement is combined with state-of-the-art CMB measurements. Allowing the effective number of neutrinos to vary as a free parameter does not significantly change these results. When we combine the measurement of $f^{0.43}\sigma_8$ with the complementary measurement of $f\sigma_8$ from the monopole and quadrupole of the two-point correlation function we are able to obtain an independent measurements of f and σ_8 . We obtain $f = 0.63 \pm 0.16$ and $\sigma_8 = 0.710 \pm 0.086$ (68% confidence level). This is the first time when these parameters have been able to be measured independently using this methodology from galaxy clustering data only.

Key words: cosmology: theory - cosmology: cosmological parameters - cosmology: large-scale structure of Universe - galaxies: haloes

1 INTRODUCTION

Direct and model-independent constraints on the growth of cosmological structure are particularly important in cosmology. Measurements of the expansion history of the Universe (via standard candles or standard rulers) have clearly indicated an accelerated expansion since redshift $z \sim 0.3$, but are insufficient to identify the physics causing it; information

on the growth of structure is key (for a review of the state of the field and general introduction to it see e.g., Albrecht et al. (2006); Amendola et al. (2013); Feng et al. (2014) and references therein). In particular, while the cosmological constant remains at the core of the standard cosmological model, and is the most popular explanation for the accelerated expansion, it raises several problems from its smallness (the cosmological constant problem) to its fine tuning (the coincidence problem). This situation has led many scientists to investigate alternative forms of vacuum energy (dark en-

* hector.gil@port.ac.uk

ergy) or to challenge one of the basic tenets of cosmology, namely General Relativity (GR). After all, precision tests of GR have been performed on solar system scales, but more than 10 orders of magnitude extrapolation is required to apply it on cosmological scales. Should GR be modified on cosmological scales, it could still mimic the Λ CDM expansion history but the growth of structure would be affected.

Most of the information we can gather about clustering and large scale structure, which on large scales would trace the linear growth of perturbations, come from galaxies. It is well known that different kinds of galaxies show different clustering properties, and thus not all objects can be faithful tracers of the underlying mass distribution; this feature is called galaxy bias. There are two notable observational techniques that avoid this limitation: gravitational lensing and redshift-space distortions. Gravitational lensing is an extremely promising approach which, however, at present reaches limited signal-to-noise ratio in the linear or mildly non-linear regime. The study of redshift-space distortions observed in galaxy redshift surveys uses galaxies as test particles in the velocity field and thus this technique is relatively insensitive to galaxy bias¹.

A third approach is to use higher-order correlations to disentangle the effects of gravity from those of galaxy bias (e.g., Fry 1994). This is the approach recently pursued in Gil-Marín et al. (2014) where, by performing a joint analysis of the monopole power spectrum and bispectrum of the CMASS sample of the Baryon Oscillation Spectroscopic Survey Data Release 11 (BOSS DR11 SDSSIII) survey (Gunn et al. 1998, 2006; Eisenstein et al. 2011; Bolton et al. 2012; Dawson et al. 2013; Smee et al. 2013), constraints on both galaxy bias and growth of structures at the effective redshift of the survey $z = 0.57$ were obtained.

Here we investigate the cosmological implications of the measurement of the quantity $f^{0.43}\sigma_8$ at $z = 0.57$ (hereafter $f^{0.43}\sigma_8|_{z=0.57}$) obtained in Gil-Marín et al. (2014) (hereafter Paper I). The parameter f quantifies the linear growth rate of structures: $f = d\ln\delta/d\ln a$, where a is the scale factor and δ the (linear) matter overdensity fluctuation; σ_8 is the *rms* of the (linear) matter overdensity field extrapolated at $z = 0$ and smoothed on scales of $8 h^{-1}\text{Mpc}$. Paper I reported $f^{0.43}\sigma_8|_{z=0.57} = 0.582 \pm 0.084$ (0.584 ± 0.051); where the first result correspond to the conservative analysis while the second to the more optimistic analysis (see Gil-Marín et al. (2014) for details). Hereafter we report in parenthesis the results corresponding to the optimistic analysis. The difference in the central values is negligible at all effects thus we will only report the error-bars corresponding to the optimistic analysis. This 14% (9%) error on the quantity $f^{0.43}\sigma_8|_{z=0.57}$ is comparable to that obtained in the quantity $f\sigma_8$ from the study of redshift-space distortions of the power spectrum of the same survey (e.g., Beutler et al. 2013; Chuang et al. 2013; Samushia et al. 2014 and Sánchez et al. 2014), which have error-bars of typically 10%. While not being statistically independent (the survey is the same), the method is complementary and the measurement relies on

a different physical effect, harvesting the power of higher-order correlations rather than the anisotropy of clustering induced by the redshift-space distortions. This paper is organised as follows: in § 2 we present the data sets we use and the methodology. § 3 tests first the consistency of the measurement with the Λ CDM model with GR, then proceeds in constraining several extensions of this model which involve changes in the composition (i.e., neutrino properties) or background (i.e., dark energy models and geometry) or deviations from GR. We explore the potential of combining the bispectrum monopole with anisotropic clustering of the two point function in § 4. and conclude in § 5.

2 METHODS AND DATA SETS

In Paper I we have analysed the anisotropic clustering of the Baryon Oscillation Spectroscopic Survey (BOSS) CMASS Data Release 11 sample, composed of 690827 galaxies in the redshift range of $0.43 < z < 0.70$. This survey covers an angular area of 8498 deg^2 , which corresponds to an effective volume of $\sim 6 \text{ Gpc}^3$. We have measured the corresponding redshift-space galaxy power spectrum and bispectrum monopoles, providing a measurement of the linear growth rate, f , in combination with the amplitude of matter density fluctuations, σ_8 , $f^{0.43}\sigma_8 = 0.582 \pm 0.084$ (0.584 ± 0.051) at the effective redshift of the survey, $z_{\text{eff}} = 0.57$. The optimistic estimate is obtained by pushing slightly more into the mildly non-linear regime and thus including significantly more modes. For this particular combination of f and σ_8 , close to the maximum likelihood solution the likelihood surface is much closer to that of Gaussian distribution than in the individual parameters. In addition, this measurement is insensitive to the fiducial cosmology assumed in the analysis. We have performed a series of detailed systematic tests based on galaxy mocks and N-body simulations, which demonstrate the robustness of the result. The statistical error on $f^{0.43}\sigma_8|_{z=0.57}$ has been obtained from the scatter among 600 mock catalogs: this enables a reliable estimate of the 68% (1- σ) confidence, but we cannot reliably explore the wings of the distribution. Here we adopt a Gaussian distribution of the uncertainty.

We combine the $f^{0.43}\sigma_8|_{z=0.57}$ measurement with the constraints from Cosmic Microwave Background (CMB) observations acquired by the *Planck* satellite (Planck Collaboration et al. 2011, 2013a,b). In many cases we use the outputs of their Monte Carlo Markov Chains for importance sampling; when specified we run new Markov chains. We use either the *Planck* + *WP* data – *Planck* primary temperature data with the Wilkinson Microwave Anisotropy Probe WMAP (Bennett et al. 2003) polarisation data (Bennett et al. 2012; Hinshaw et al. 2012) at low multipoles – or *Planck* + *WP* + *highL* – the above data with the addition of high multipoles temperature observations from the Atacama Cosmology Telescope (Das et al. 2013) and the South Pole telescope (Reichardt et al. 2012). The *Planck* maps have also been analysed to extract the weak gravitational lensing signal arising from intervening large scale structure (Planck Collaboration et al. 2013c). This task is done through the four point function of the temperature maps; when including this information we refer to it as *lensing*. In some cases the CMB constraints are improved by the addition of infor-

¹ This technique would be sensitive, of course, to a velocity bias if tracers did not to statistically represent the distribution of velocities of dark matter. Such a velocity bias is not expected on large-scales.

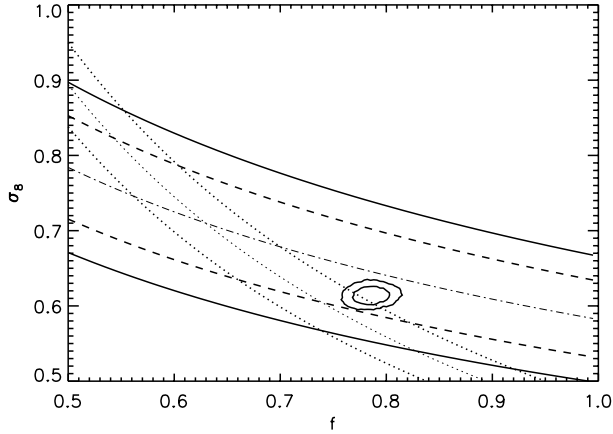


Figure 1. Constraints in the f - σ_8 plane where both quantities are at the effective redshift of the BOSS CMASS DR11 galaxies $z = 0.57$. The ellipses represent the *Planck* CMB inferred constraints (68 and 95% confidence) when assuming GR and a Λ CDM model. The dot-dashed line represents the best-fitting value for the measurements of Paper I, which uses the monopole power spectrum and bispectrum of the BOSS CMASS DR11 galaxies. The solid and dashed lines represent the 68% confidence region corresponding to the conservative and optimistic analysis respectively. The dotted lines are the 68% constraints obtained from the monopole and quadrupole of the two-point function from the same galaxy catalog (Samushia et al. 2014).

mation on the expansion history via Baryon Acoustic Oscillation (BAO) measurements (Beutler et al. 2011; Blake et al. 2011; Padmanabhan et al. 2012; Anderson et al. 2013; Percival et al. 2010).

In § 4 we also consider the measurement of the combination $f\sigma_8$ from Samushia et al. (2014). This reference uses the same data set as Paper I but exploits the fact that redshift-space distortions cause an isotropic two-point correlation function become anisotropic. The magnitude of the large-scale velocity field traced by galaxies depends on the nature of gravitational interactions, thus the angular dependence of the two-point function can be used to measure the combination $f\sigma_8$. For more details see Reid et al. (2012); Samushia et al. (2014) and references therein.

3 RESULTS

We start by investigating whether the $f^{0.43}\sigma_8|_{z=0.57}$ measurement is consistent with the Λ CDM+GR model prediction when the model parameters are constrained by CMB observations. Assuming GR, the expansion history uniquely predicts the linear growth rate. In a Λ CDM+GR model, observations of the CMB impose tight constraints on the expansion history and therefore on the growth of structure.

Fig. 1 presents the constraints on the f - σ_8 -plane, at $z = 0.57$, obtained from the *Planck*+*WP* CMB observations extrapolated assuming GR and a flat- Λ CDM model, from the direct measurement of Paper I and, for completeness, from the BOSS CMASS galaxies anisotropic clustering (Samushia et al. 2014): $f\sigma_8 = 0.447 \pm 0.028$, at $z = 0.57$.

The galaxy clustering measurements are in agreement with the standard Λ CDM cosmological paradigm.

As the two measurements constrain different combinations of f and σ_8 , both to be measured separately from a combined analysis. We explore this prospect in § 4.

Although there is no evidence for significant tensions between the CMB and the lower redshift measurements, we now consider standard Λ CDM model extensions, where one or more extra cosmological parameters are allowed to vary. We then consider direct constraints on modifications of GR.

3.1 Neutrino mass constraints

Among possible Λ CDM model extensions, which still assume GR, we expect the $f^{0.43}\sigma_8|_{z=0.57}$ measurement to provide significant improvement over CMB data alone for the cases of where significant evolution in the growth rate to low redshift is expected. This is the case for massive neutrinos and for models where dark energy deviates from a cosmological constant and where more than one evolution-affecting parameter is added to the “base” Λ CDM model. In other model extensions, the addition of the growth constraints only reduces the CMB error-bars by few percent. In these cases therefore, this combination offers a test of consistency rather than a technique of reducing parameter degeneracies and improving cosmological constraints.

Massive neutrinos affect the growth of cosmological structure by suppressing clustering below their free streaming length; as a result in models with massive neutrinos the power spectrum amplitude at large-scale structure scales is lower than that at CMB scales. If we allow the three standard-model neutrinos to have a non-zero mass and the sum of the masses m_ν to be the parameter to be constrained, the *Planck*+*WP* data constraints are $m_\nu < 1.31$ eV at 95% confidence, which become $m_\nu < 0.66$ eV when the *highL* data are considered. Including the $f^{0.43}\sigma_8|_{z=0.57}$ measurement produces $m_\nu < 0.68(0.47)$ eV and $m_\nu < 0.49(0.38)$ eV, respectively, always at 95% confidence, which represent a factor 2 (2.8) and 1.3 (1.7) improvement, respectively. When the information about lensing is included (through the four point function of the CMB temperature) in the CMB analysis the constraint on neutrino masses relaxes to, $m_\nu < 0.85$ eV (95% confidence)². Including $f^{0.43}\sigma_8|_{z=0.57}$ brings back the upper limit to $m_\nu < 0.67(0.50)$ eV. Fig. 2 presents the constraints in the σ_8 - m_ν plane and illustrates the above features. Basically the $f^{0.43}\sigma_8|_{z=0.57}$ measurement, by effectively constraining σ_8 , breaks the m_ν - σ_8 degeneracy.

A slightly more general extension of the Λ CDM model is the case where both the number of effective neutrino species N_{eff} and the neutrino mass m_ν are treated as free parameters. Also in this case the $f^{0.43}\sigma_8|_{z=0.57}$ measurement improves the constraints, especially on the sum of neutrino masses. This behaviour is illustrated in Fig. 3, where the blue, dashed contours are for *Planck*+*WP* and the solid, thick purple (thin, black) contours are in combination with the $f^{0.43}\sigma_8|_{z=0.57}$ measurement. For m_ν (marginalised over

² This point is discussed at length in the literature and in Planck Collaboration et al. (2013b) and is possibly due to a mild tension between the CMB damping tail and the four-point function constraints on the magnitude of the lensing signal.

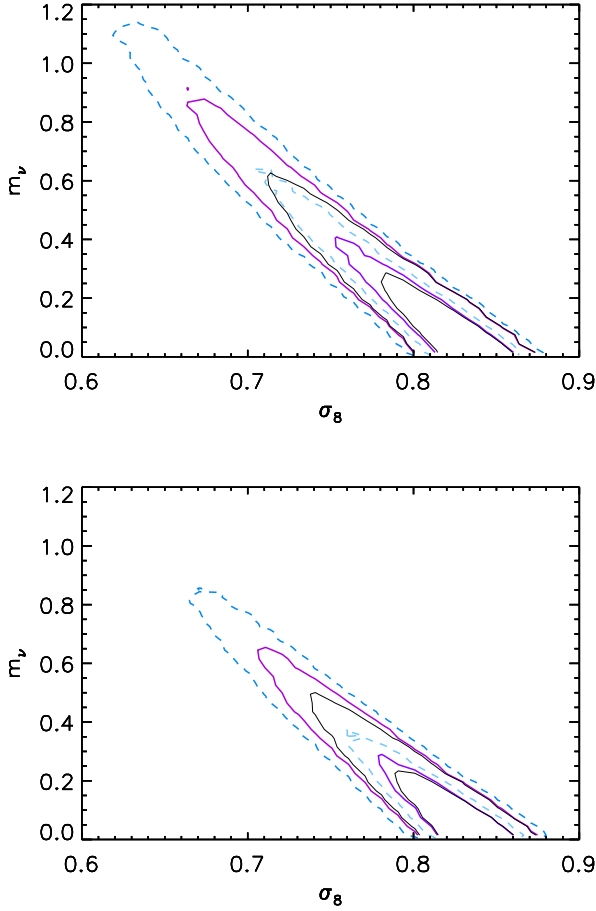


Figure 2. Constraints in the σ_8 – m_ν plane. In both panels the blue, dashed contours are the (joint) 68 and 95% confidence regions for *Planck*. On the top panel *Planck* temperature data and WMAP low ℓ polarisation are used (*Planck* + *WP*), while on the bottom panel also the *highL* data are included (*Planck* + *WP* + *highL*). The solid contours show how constraints improve by including $f^{0.43}\sigma_8|_{z=0.57}$: thick, purple lines correspond to the conservative estimate and thin, black lines to the optimistic one.

N_{eff}) the CMB constraint $m_\nu < 0.85$ eV (at 95% confidence) becomes $m_\nu < 0.63(0.46)$ eV (at 95% confidence).

Qualitatively similar results are also obtained for the massive sterile neutrino case, where the extra sterile neutrinos are made massive rather than having the mass being equally distributed among all neutrino families: $m_\nu < 0.51(0.42)$ eV at 95% confidence when we impose a limit to the physical thermal mass for the sterile neutrino < 10 eV, for which the particles are distinct from cold or warm dark matter (see Table 1 for details). Some large-scale structure datasets, including the cluster abundance from the *Planck* Sunyaev-Zeldovich clusters (Planck Collaboration et al. 2013d), yield a much lower value for $\sigma_8(z=0)$ than that inferred from the CMB assuming a standard Λ CDM-model with near massless neutrinos. This mismatch has been interpreted as an evidence of non-zero neutrino mass with $m_\nu \sim 0.45$ eV. In particular the joint analysis of *Planck* temperature data with the cluster abundance from the *Planck* Sunyaev-Zeldovich clusters (Planck Collabora-

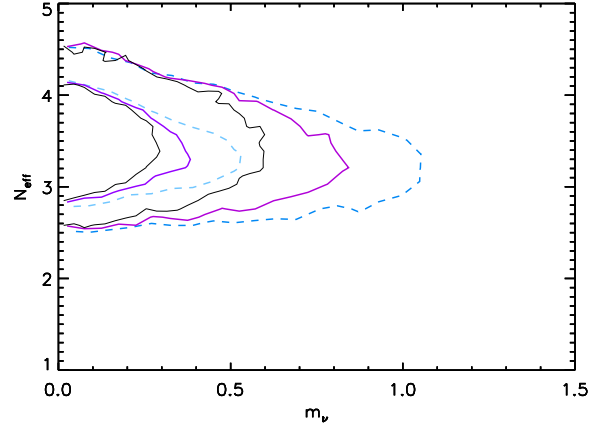


Figure 3. Constraints in the total neutrino mass m_ν , number of effective neutrino species N_{eff} from *Planck*+*WP* in (light) blue, dashed lines indicating 68% and 95% and with the addition of the $f^{0.43}\sigma_8|_{z=0.57}$ constraints in solid thick purple (solid thin black) contours. As above the tighter constraints are obtained with the optimistic measurement. For m_ν (marginalised over N_{eff}) we obtain that the CMB constraint $m_\nu < 0.85$ eV (at 95% confidence) becomes $m_\nu < 0.63(0.46)$ eV (at 95% confidence).

tion et al. 2013d) yields a tentative detection of neutrino masses $m_\nu = 0.45 - 0.58 \pm 0.21$ eV depending on assumptions about the calibration of the mass-observable relation. The $f^{0.43}\sigma_8|_{z=0.57}$ measurement seems to disfavour the “new physics in the neutrino sector” interpretation of the σ_8 mismatch. These results are summarised in Table 1.

3.2 Dark energy equation of state constraints

In the case of a non-flat model where the dark energy equation of state parameter w is constant, but not necessarily equal to -1 ($-ow$ CDM), the combination of *Planck*+*WP* and $f^{0.43}\sigma_8|_{z=0.57}$ measurements constrain w to be $-2.10 < w < -0.33$ ($-1.94 < w < -0.62$) at 95% confidence and the curvature to be $-0.093 < \Omega_k < +0.008$ ($-0.076 < \Omega_k < +0.007$), also at 95% confidence. The joint constraints in the Ω_k – w plane are displayed in the left panel of Fig. 4.

Conversely, if we assume flat geometry, but allow the dark energy equation of state to change with the scale-factor a (according to Chevallier & Polarski 2001 and Linder 2003) as $w(a) = w + w_a(1 - a)$ ($-ww_a$ CDM), we obtain the constraints presented in the middle panel of Fig. 4. The single parameter constraints are: $-2.03 < w < -0.06$ ($-1.80 < w < -0.16$) and $w_a < 1.27(1.08)$ (at 95% confidence). These constraints do not degrade significantly if flatness is relaxed ($-oww_a$ CDM), as shown in the right panel of Fig. 4. In this case the constraint on the geometry becomes $-0.083 < \Omega_k < 0.007$ ($-0.074 < \Omega_k < 0.007$) at 95% confidence and for the dark energy parameters $-2.38 < w < 0.39$ ($-2.20 < w < -0.01$) and $w_a < 1.64(1.60)$ (95% confidence). For all these cases, we ran new Markov Chains rather than importance sampling existing ones. We conclude that a dark energy component is needed and is dominant even in non-flat models where the dark energy equation of state

	$m_\nu - \Lambda\text{CDM}$			$N_{\text{eff}} - m_\nu - \Lambda\text{CDM}$	$N_{\text{eff}} - m_{\text{eff}}^{\text{sterile}} - \Lambda\text{CDM}$
	<i>Planck</i> + WP $m_\nu < 1.31 \text{ eV}$	<i>Planck</i> + WP+highL $m_\nu < 0.66 \text{ eV}$	<i>Planck</i> + WP+highL+lensing $m_\nu < 0.85 \text{ eV}$	<i>Planck</i> +WP $m_\nu < 0.85 \text{ eV}$	<i>Planck</i> + WP+highL $m_\nu < 0.59 \text{ eV}$
	$+f^{0.43}\sigma_8 _{z=0.57}$	$+f^{0.43}\sigma_8 _{z=0.57}$	$+f^{0.43}\sigma_8 _{z=0.57}$	$+f^{0.43}\sigma_8 _{z=0.57}$	$+f^{0.43}\sigma_8 _{z=0.57}$
conserv.	$m_\nu < 0.68 \text{ eV}$	$m_\nu < 0.49 \text{ eV}$	$m_\nu < 0.67 \text{ eV}$	$m_\nu < 0.63 \text{ eV}$	$m_\nu < 0.51 \text{ eV}$
optim.	$m_\nu < 0.46 \text{ eV}$	$m_\nu < 0.38 \text{ eV}$	$m_\nu < 0.50 \text{ eV}$	$m_\nu < 0.46 \text{ eV}$	$m_\nu < 0.42 \text{ eV}$

Table 1. Constraints (95% limits) on the sum of neutrino masses for several models and data set combinations. The $m_\nu - \Lambda\text{CDM}$ model is a spatially flat power law ΛCDM model where the sum of neutrino masses is an extra parameter. The $N_{\text{eff}} - m_\nu - \Lambda\text{CDM}$ model is a spatially flat power law ΛCDM model where both the effective number of neutrino species and the total neutrino mass are extra parameters. The $N_{\text{eff}} - m_{\text{eff}}^{\text{sterile}} - \Lambda\text{CDM}$ model is similar to $N_{\text{eff}} - m_\nu - \Lambda\text{CDM}$, but where the massive neutrinos are only the sterile ones. To calculate the constraints we have imposed a physical thermal mass for the sterile neutrino $< 10 \text{ eV}$, which defines the region (for the CMB) where the particles are distinct from cold or warm dark matter.

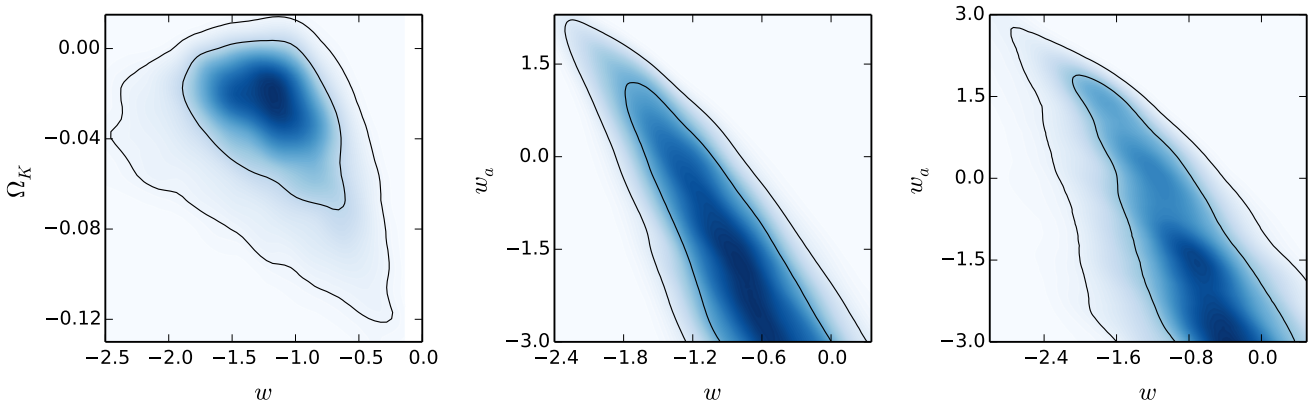


Figure 4. Constraints obtained from *Planck*+WP in combination with the $f^{0.43}\sigma_8|_{z=0.57}$ measurement for the following models. In the left panel constraints in the Ω_k - w plane for a non-flat Universe where the dark energy equation of state is constant but not necessarily -1 ; in the middle panel constraints in the w - w_a plane for a flat model where the dark energy equation of state parameter changes with the scale factor a as $w(a) = w + w_a(1 - a)$. The right panel is the same as the middle panel but where the spatial flatness assumption is relaxed. In this case $-0.076 < \Omega_k < 0.009$ (95% confidence), respectively. The contour lines represent the 68% and the 95% confidence regions. The saturation of the colour is proportional to the posterior likelihood.

parameter is not necessarily constant. The density of dark energy in units of the critical density $\Omega_{\text{dark energy}}$ at 68% confidence is 0.61 ± 0.13 (0.637 ± 0.090) in the $ow\text{CDM}$ model, 0.742 ± 0.071 (0.728 ± 0.055) in the $ww_a\text{CDM}$ model and 0.62 ± 0.12 (0.639 ± 0.086) in the $oww_a\text{CDM}$ model. These constraints are obtained using only data at $z \geq 0.57$ (i.e., $f^{0.43}\sigma_8|_{z=0.57}$ and CMB). Any more “local” explanation for dark energy is therefore disfavoured.

3.3 Modifications of GR

In modern cosmology the rationale behind introducing modifications of GR is to explain the late-time cosmological acceleration. Therefore, the most popular modifications of GR mimic the effects of the cosmological constant on the expansion history and become important only at low redshifts. If we allow gravity to deviate from GR, the CMB offers only weak constraints on the late-time growth of structures, via the Integrated Sachs-Wolfe (ISW) effect and lensing. A popular parametrisation for deviations from GR growth is given by,

$$f(z) = \Omega_m(z)^\gamma. \quad (1)$$

For $\Lambda\text{CDM}+\text{GR}$ $\gamma|_{\Lambda\text{CDM}} \simeq 0.56$; for dark energy models with an equation of state parameter different from $w = -1$, γ acquires a weak redshift dependence and its value does not deviate significantly from $\gamma|_{\Lambda\text{CDM}}$. Since we have a measurement at a given redshift we consider γ to be constant. We also assume that this modification affects the late-time Universe and not the CMB. This assumption is reasonable as in this parametrisation, as $\Omega_m(z) \rightarrow 1$ (i.e., for most cosmologies at $z \gg 1$) the growth becomes that of an Einstein-De-Sitter Universe for any value of γ .

For this extension to the base model we assume that the background expansion history is given by that of the ΛCDM -model as constrained by *Planck*+WP (using *Planck*+WP+highL+BAO does not change the results significantly). The constraints on the growth rate reduce to $\gamma = 0.40^{+0.50}_{-0.26}$ at 68% confidence and $\gamma < 0.87$ (0.80) at 95% confidence.

For coupled dark energy-dark matter models the growth can be parametrised as (e.g., di Porto & Amendola (2008) and references therein),

$$f(z) = \Omega_m(z)^{0.56}(1 + \eta). \quad (2)$$

Using this equation we obtain $\eta = 0.055 \pm 0.145$ (± 0.090)

at 68% confidence. For the coupled dark energy-dark matter models, η is related to the coupling constant β_c . These models have a non-negligible amount of dark energy at early times, so they can be constrained by the CMB. Nevertheless, the η constraint can be re-interpreted as a limit on the coupling constant $\beta_c < 0.34$ (< 0.28) at 95% confidence at the effective survey redshift $z = 0.57$; as expected this constraint is much weaker than that obtained from the CMB by Pettorino et al. (2012) assuming a constant coupling.

Inspired by Acquaviva et al. (2008), who introduced the quantity $\epsilon = f/f|_{\Lambda\text{CDM}} - 1$, we can define

$$\epsilon' \equiv \frac{f^{0.43}\sigma_8}{f^{0.43}\sigma_8|_{\Lambda\text{CDM}}} - 1, \quad (3)$$

which is a more model-independent approach than the γ -parameterisation of Eq. 1 and that enables one to quantify possible late-time deviations from GR. This quantity, which is identical to zero for ΛCDM and exceedingly close to zero for minimally coupled quintessence-type models, is redshift dependent and can, in principle, be also scale dependent when departures from GR are present. Here we assume ϵ' is scale-independent over the scales probed and we compute its value at the effective survey redshift. For $f^{0.43}\sigma_8|_{\Lambda\text{CDM}}$ we take the range predicted by the *Planck*+*WP* combination and obtain, at 68% confidence,

$$\epsilon'(z = 0.57) = 0.04 \pm 0.15(\pm 0.10), \quad (4)$$

in agreement with the GR value of zero.

4 BREAKING THE f - σ_8 DEGENERACY

As displayed in Fig. 1, the constraints in the $f - \sigma_8$ plane produced by the redshift-space distortions of the anisotropic redshift-space correlation function and those produced by the monopole of the power spectrum and bispectrum are highly complementary.

A joint analysis combining the two-point anisotropic clustering and the bispectrum monopole is able to break the degeneracy between f and σ_8 , enabling the measurement of both quantities separately. Here we do not attempt a full, combined analysis of the power spectrum monopole, quadrupole and the bispectrum monopole, which would yield the combined constraint of multiples parameters, including bias if a single consistent bias model were adopted. We will consider such analysis in a future work.

Instead, we perform a combined, *a posteriori*, analysis between the measurements of $f\sigma_8|_{z=0.57}$ obtained by Samushia et al. (2014), when the background expansion is fixed to the one predicted by Planck, and of $f^{0.43}\sigma_8|_{z=0.57}$ obtained in Paper I. Although the measurements were carried out independently, and one is performed in configuration space while the other in Fourier space, they share the information related to the monopole of the two-point statistics, and therefore they are expected to be moderately correlated. Using measurements based on the same set of mocks (Manera et al. 2013) we compute the correlation and errors from their dispersion (see § 3.9 in Paper I for details of the method). We consider the measurement of $[f\sigma_8]_i$ and $[f^{0.43}\sigma_8]_i$ for each single i -mock, and combining them we

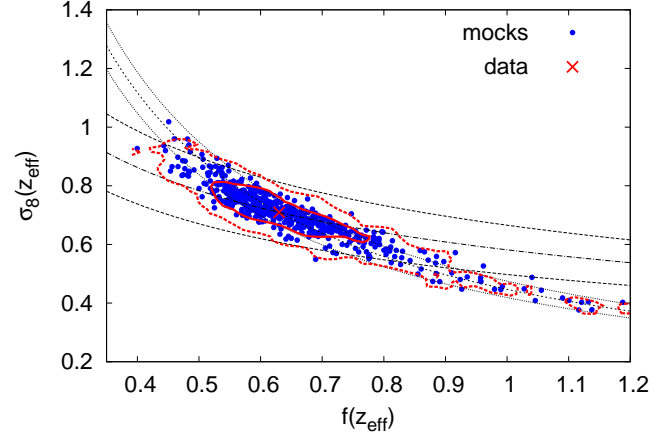


Figure 5. Constraints in the f - σ_8 plane where both quantities are at the effective redshift of the BOSS CMASS DR11 galaxies $z = 0.57$. In this figure, for $f^{0.43}\sigma_8|_{z=0.57}$ we consider the conservative measurement only. The blue circles represent the best-fitting values for 600 mocks when the results from Samushia et al. (2014) (short dashed line) and Paper I (dot-dashed line) are combined (see text for details). The dotted lines and the dashed lines show the 1σ errors, respectively. The contours correspond to the 68 and 95% confidence regions (solid and dashed lines, respectively) estimated from the dispersion of the mocks. The red cross represents the best-fitting value for the BOSS CMASS DR11 data. The best-fitting values of the galaxy mocks, as well as the contours, have been displaced in the logarithmic space to be centered on the measurement from the data.

extract the corresponding values:

$$[f]_i = \{[f\sigma_8]_i/[f^{0.43}\sigma_8]_i\}^{1/0.57}, \quad (5)$$

$$[\sigma_8]_i = [f\sigma_8]_i/[f]_i. \quad (6)$$

The errors on f and σ_8 are estimated from the dispersion of $[f]_i$ and $[\sigma_8]_i$ among all the mocks, respectively. This result is illustrated in Fig. 5, where the blue circles represent the obtained values of $[f]_i$ and $[\sigma_8]_i$ for the 600 realisations of the galaxy mocks: $i = 1, 2, \dots, 600$.

The combined constraints in the $f - \sigma_8$ plane are displayed in Fig. 5, which illustrates the constraints on $f\sigma_8$ and $f^{0.43}\sigma_8$ from Samushia et al. (2014) and Paper I, respectively, using the same line-notation as in Fig. 1. Blue circles represent the best-fit values for the mocks and the red cross shows the best-fit value for the DR11 CMASS dataset. The contours correspond to the 68% (solid lines) and 95% (dashed lines) confidence levels extracted from the mocks and centered on the data, where the mild prior $0 < f < 2$ has been used.

Originally the constraints on $f\sigma_8$ and $f^{0.43}\sigma_8$ were: $f\sigma_8|_{z=0.57} = 0.447 \pm 0.028$ and $f^{0.43}\sigma_8|_{z=0.57} = 0.582 \pm 0.084$ (0.051). After combining the measurements, we obtain $f(z_{\text{eff}}) = 0.63 \pm 0.16$ (0.13), $\sigma_8(z_{\text{eff}}) = 0.710 \pm 0.086$ (0.069), where all the reported errors are at the 68% confidence level. These values represent a 12(10)% and 25(20)% relative error for $\sigma_8(z_{\text{eff}})$ and $f(z_{\text{eff}})$, respectively. This is the first time that these two quantities have been separately measured from galaxy clustering using this methodology.

The resulting values for f and σ_8 are in broad agreement with the CMB-inferred values. We have repeated the analysis of § 3.1 and 3.2 using these new constraints, but we find that the constraints on the cosmological parameters do not change in any significant way. At the current size of the error-bars of $f^{0.43}\sigma_8|_{z=0.57}$, the $f\sigma_8$ degeneracy is being cut for high values of σ_8 , but has a tail for low values of σ_8 , as it is shown in Fig. 5. Therefore, breaking the $f\sigma_8$ degeneracy in this way (in combination with Planck data) does not improve significantly the error-bars in the studied parameters. We expect that this will improve with the forthcoming analysis of DR12, where a joint analysis of power spectrum monopole, quadrupole and bispectrum monopole will be performed.

When the measurements obtained on f are applied to the parameters of Eq. 1 the constraints on γ become $\gamma = 0.40 \pm 0.43(0.35)$ (68% confidence). We can now consider the variable ϵ introduced by Acquaviva et al. (2008), obtaining $\epsilon = -0.21 \pm 0.56(0.45)$, also at 68% confidence. Both measurements should be considered at $z_{\text{eff}} = 0.57$ at scales of $k \simeq 0.1 h\text{Mpc}^{-1}$. In order to be able to use these measurements to distinguish between GR and popular and viable modifications of gravity that match the ΛCDM model expansion history, error-bars would have to be reduced by a factor of few.

5 CONCLUSIONS

We have examined the cosmological implications of the constraints on the quantity $f^{0.43}\sigma_8$ at $z_{\text{eff}} = 0.57$, which offers a direct cosmological and model-independent probe of the growth of structure. This constraint has been obtained from the measurement of the power spectrum and bispectrum monopoles of the SDSSIII BOSS DR11 CMASS galaxies and has been recently presented in a companion paper (Gil-Marín et al. 2014) (Paper I).

We have combined this result with recent state-of-the-art CMB constraints for several underlying cosmological models. We find agreement in the standard ΛCDM cosmological paradigm between the growth of structure predicted by CMB observations and the direct measurement from galaxy clustering.

When considering popular ΛCDM model extensions, which still rely on GR, we find that this new measurement is useful to improve the CMB constraints on cosmological parameters only for model extensions that involve massive neutrinos or for models where dark energy deviates from a cosmological constant and where more than one parameter is added. The $f^{0.43}\sigma_8|_{z=0.57}$ measurement improves CMB neutrino mass constraints by at least 30% and in some cases by as much as factor 2 to 2.8. (see Table 1 for details). There is no evidence for non-standard neutrino properties when considering CMB and $f^{0.43}\sigma_8|_{z=0.57}$ measurements.

For dark energy models where the equation of state parameter of dark energy is not constant, or for models where it is constant but not equal to -1 and the geometry of the Universe is not constrained to be flat, we can obtain interesting constraints. Curvature is constrained at the 8% level (95% confidence). We find no evidence for any deviations from a cosmological constant, but dark energy is needed as a dominant component of the Universe, even for non-flat,

non- ΛCDM cosmologies. This conclusion is reached using only data at $z \geq 0.57$, thus disfavouring “local” explanations of dark energy.

We have also examined the constraints that the measurement of $f^{0.43}\sigma_8|_{z=0.57}$, in combination with data on the Universe’s geometry and expansion history, provide on modifications of GR. We have examined different phenomenological parametrisations of how the growth of structure is modified when we relax the assumption of GR. We do not observe any significant tension between these measurements and GR predictions, in particular we find that $\gamma = 0.40^{+0.50}_{-0.45}({}^{+0.28}_{-0.26})$ (68% confidence), where $f(z) = \Omega_m(z)^\gamma$.

Finally, we have presented how the measurement of $f^{0.43}\sigma_8|_{z=0.57}$ can be combined with the measurement of $f\sigma_8|_{z=0.57}$ from the same galaxy sample to break the degeneracy between f and σ_8 . This is the first time that a separate measurement of f and σ_8 has been obtained using this methodology from galaxy clustering: $f = 0.63 \pm 0.16$ and $\sigma_8 = 0.710 \pm 0.086$, both at $z = 0.57$. The size of errors already provides an insight on how powerful a fully and optimal joint analysis can be. We find that f can be measured with a relative precision of $\sim 25\%$, and σ_8 with $\sim 10\%$ at 68% confidence level. We expect that the size of these error-bars can be reduced if the power spectrum multipoles and bispectrum monopole are combined *prior* to obtain the f and σ_8 best-fitting values. Further testing for potential systematics would also be of benefit for such novel analysis.

While the $f - \sigma_8$ degeneracy could also be broken using measurements at several different redshifts, or resorting to weak lensing data or cross correlation with the weak lensing signal of the CMB, the approach described in this paper provides a complementary and self-contained approach to achieve the same goal relying on galaxy redshift surveys alone, without the need of wide redshift coverage.

ACKNOWLEDGEMENTS

HGM is grateful for support from the UK Science and Technology Facilities Council through the grant ST/I001204/1. LV is supported by the European Research Council under the European Community’s Seventh Framework Programme grant FP7-IDEAS-Phys.LSS and acknowledges Mineco grant FPA2011-29678-C02-02. JN is supported in part by ERC grant FP7-IDEAS-Phys.LSS. AC is supported by the European Research Council under the European Community’s Seventh Framework Programme grant FP7-IDEAS-Phys.LSS. WJP is grateful for support from the UK Science and Technology Facilities Research Council through the grant ST/I001204/1, and the European Research Council through the grant “Darksurvey”.

Funding for SDSS-III has been provided by the Alfred P. Sloan Foundation, the Participating Institutions, the National Science Foundation, and the U.S. Department of Energy Office of Science. The SDSS-III web site is <http://www.sdss3.org/>.

SDSS-III is managed by the Astrophysical Research Consortium for the Participating Institutions of the SDSS-III Collaboration including the University of Arizona, the Brazilian Participation Group, Brookhaven National Laboratory, University of Cambridge, Carnegie Mellon University, University of Florida, the French Participation

Group, the German Participation Group, Harvard University, the Instituto de Astrofísica de Canarias, the Michigan State/Notre Dame/JINA Participation Group, Johns Hopkins University, Lawrence Berkeley National Laboratory, Max Planck Institute for Astrophysics, Max Planck Institute for Extraterrestrial Physics, New Mexico State University, New York University, Ohio State University, Pennsylvania State University, University of Portsmouth, Princeton University, the Spanish Participation Group, University of Tokyo, University of Utah, Vanderbilt University, University of Virginia, University of Washington, and Yale University. This research used resources of the National Energy Research Scientific Computing Center, which is supported by the Office of Science of the U.S. Department of Energy under Contract No. DE-AC02-05CH11231.

Results are based on observations obtained with Planck (<http://www.esa.int/Planck>), an ESA science mission with instruments and contributions directly funded by ESA Member States, NASA, and Canada.

Numerical computations were done on Hipatia ICC-UB BULLx High Performance Computing Cluster at the University of Barcelona.

REFERENCES

- Acquaviva V., Hajian A., Spergel D. N., Das S., 2008, *Phys. Rev. D*, 78, 043514
- Albrecht A. et al., 2006, ArXiv Astrophysics e-prints
- Amendola L. et al., 2013, *Living Reviews in Relativity*, 16, 6
- Anderson L., Aubourg E., Bailey S., Bizyaev D., Blanton M., et al., 2013, *Mon.Not.Roy.Astron.Soc.*, 427, 3435
- Bennett C., Larson D., Weiland J., Jarosik N., Hinshaw G., et al., 2012
- Bennett C. L. et al., 2003, *ApJS*, 148, 1
- Beutler F., Blake C., Colless M., Jones D. H., Staveley-Smith L., et al., 2011, *Mon.Not.Roy.Astron.Soc.*, 416, 3017
- Beutler F. et al., 2013, ArXiv e-prints
- Blake C., Kazin E., Beutler F., Davis T., Parkinson D., et al., 2011, *Mon.Not.Roy.Astron.Soc.*, 418, 1707
- Bolton A. S. et al., 2012, *AJ*, 144, 144
- Chevallier M., Polarski D., 2001, *International Journal of Modern Physics D*, 10, 213
- Chuang C.-H. et al., 2013, *MNRAS*, 433, 3559
- Das S., Louis T., Nolte M. R., Addison G. E., Battistelli E. S., et al., 2013
- Dawson K. S. et al., 2013, *AJ*, 145, 10
- di Porto C., Amendola L., 2008, *Phys. Rev. D*, 77, 083508
- Eisenstein D. J. et al., 2011, *AJ*, 142, 72
- Feng J. L. et al., 2014, ArXiv e-prints
- Fry J. N., 1994, *Physical Review Letters*, 73, 215
- Gil-Marín H., Noreña J., Verde L., Percival W. J., Wagner C., Manera M., Schneider D. P., 2014, ArXiv e-prints
- Gunn J. E. et al., 1998, *AJ*, 116, 3040
- Gunn J. E. et al., 2006, *AJ*, 131, 2332
- Hinshaw G., et al., 2012
- Linder E. V., 2003, *Physical Review Letters*, 90, 091301
- Manera M. et al., 2013, *MNRAS*, 428, 1036
- Padmanabhan N., Xu X., Eisenstein D. J., Scalzo R., Cuesta A. J., et al., 2012
- Percival W. J., et al., 2010, *Mon.Not.Roy.Astron.Soc.*, 401, 2148
- Pettorino V., Amendola L., Baccigalupi C., Quercellini C., 2012, *Phys. Rev. D*, 86, 103507
- Planck Collaboration et al., 2013a, ArXiv e-prints
- Planck Collaboration et al., 2013b, ArXiv e-prints
- Planck Collaboration et al., 2013c, ArXiv e-prints
- Planck Collaboration et al., 2013d, ArXiv e-prints
- Planck Collaboration et al., 2011, *A&A*, 536, A1
- Reichardt C., Shaw L., Zahn O., Aird K., Benson B., et al., 2012, *Astrophys.J.*, 755, 70
- Reid B. A. et al., 2012, *MNRAS*, 426, 2719
- Samushia L. et al., 2014, *MNRAS*, 439, 3504
- Sánchez A. G. et al., 2014, *MNRAS*, 440, 2692
- Smee S. A. et al., 2013, *AJ*, 146, 32